A CURRENT FIVE-LEVEL BOOST INVERTER APPLIED TO A GRID-CONNECTED PHOTOVOLTAIC SYSTEM

Márcio do C. B. Rodrigues, Estevão C. Teixeira and Henrique A. C. Braga

Núcleo de Automação e Eletrônica de Potência – NAEP
Faculdade de Engenharia – Universidade Federal de Juiz de Fora
Cx. Postal 422, 36001-970, Juiz de For a, MG, Brasil
Phone: +55 32 3229-3443 ext: 28; FAX: +55 32 3229-3401
e-mail: carmo@eletrica.ufjf.br, estevao@eletrica.ufjf.br and hbraga@engelet.ufjf.br

***Abstract* – This paper deals with the use of current multilevel converters applied to grid-connected photovoltaic systems. A brief background on the most used topologies is provided. A boost based low frequency switching converter is proposed here, which has been devised to impose a five-level, low distortion current waveform into the utility grid. Up to now, common sense and Pspice® simulation results provide strong evidences about the simplicity, reliability and the usefulness of the system when applied to either residential or higher power applications. A sinusoidal pulse-width modulation switching alternative is also presented in order to improve the current harmonic content.**

KEYWORDS

Renewable energy, PV energy processing, grid-connected PV systems, multilevel converters, multilevel PWM.

I. INTRODUCTION

During the past decades efforts have been made on searching alternatives to replace the present most important energy source: the fossil oil. The 2001 Brazilian energy crisis increased the national interest on non conventional forms of energy sources. The photovoltaic (PV) solar energy comes up as being a very interesting alternative on supplement the electric system generation. Due to the persistent cost reduction of PV panels this kind of solar energy exploitation, once attractive in the past only in remote regions or rural zones, started to become an economically-interesting alternative even in urban applications, such as small-rated single-phase residential generation units connected to the utility grid.

In a PV panel, the solar energy is directly converted into electric energy, through the photovoltaic effect, generating a dc voltage across its terminals. Thus, it is necessary a conversion stage to make it possible to inject this kind of energy into the utility grid.

By the end of 1980's, the majority of PV systems were based on line-commutated current-source inverters (CSI), employing thyristors as the main switches, as shown in Fig. 1(a) [1]. Power ratings could be of several kW. These topologies are robust, highly efficient and simple. However, such systems present a low power factor, injecting a highly distorted current with a nonzero displacement factor into the utility grid. Therefore it would be quite compulsory to repair this unacceptable condition by means of special filters and power factor compensators.

In order to improve the harmonic content and to provide a more efficient use of the PV panels, high-frequency switching became a trend in the recent years. A typical PV system employing this concept is depicted in Fig. 1 (b), which is usually applied to low power applications. The dc-to-dc converter boosts the panel voltage to proper levels and also is used to track the PV panel maximum-power point (MPP). This stage can be either a non-isolated converter, such as the boost type [2, 3], or an isolated one, such as the push-pull [4] or flyback [5]. On the other hand, the ac-to-dc conversion is usually accomplished by a voltage-source inverter (VSI), which injects a low distortion current into the grid. Switching strategy normally employs sinusoidal pulse-width modulation (PWM) [2, 3], [5 – 8]. A low-pass passive filtering is finally included at the output in order to minimize high frequency components from the injected current.

Another approach employed a dc-to-dc buck converter, switching at 20 kHz, in association with a 60 Hz CSI [4]. It is also possible to conceive a PV-to-grid system with no use of dc-to-dc converters, employing a high frequency VSI to process the energy and inject it into the utility, as shown in [7] and [8]. Low-pass filtering and a low frequency isolation transformer is also used in this case. The major drawback of the high-frequency conversion systems is that their efficiencies are lower than that of line-commutated ones, due to their higher switching losses [1].

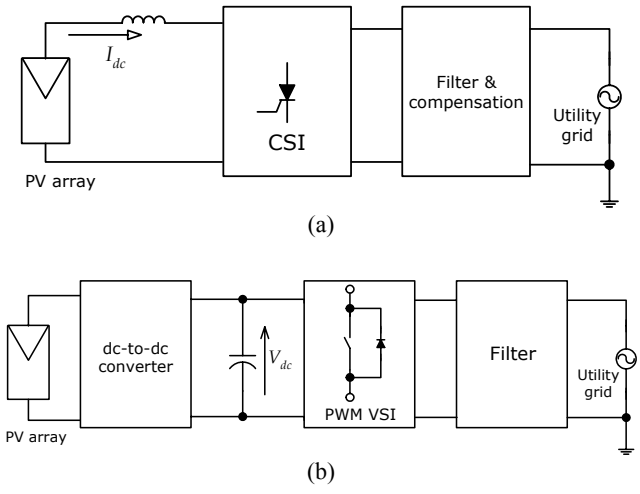

Fig. 1 – Typical photovoltaic systems topologies.
(a) Line-commutated; (b) High-frequency switching.

Some converters use soft-switching techniques to minimize these losses, but this solution results in a higher complexity for the overall system. Other common drawbacks of high-frequency systems include the need of care with parasitic elements, EMI issues and problems with the PCB layout design.

The galvanic isolation between the photovoltaic panels and the utility grid is another important issue. It can be done by means of either low-frequency [8] or high-frequency transformers [4], [5], [6]. In the latter, the transformer is a component of the isolated dc-to-dc converter. In order to reduce cost and complexity, many PV system strategies do not employ galvanic isolation [2], [3], [7]. This strategy leads to a relative difficult concerning panel earthing. Although the panel isolation is not a compulsory requirement in some standards (e. g. IEEE Std. 929-2000) [9], neither is an obligation in countries as Germany and United States, it is a necessary requirement in other ones, such as Italy and United Kingdom. Thus, there is not a uniformity regarding the isolation and earthing requirements by international standards organizations, such as IEEE and IEC, among others [1].

This paper introduces a new low-frequency current multilevel system (CML) mainly devised to provide a high efficiency system, high power factor and low total harmonic distortion (THD) of the injected current. The circuit features a relatively simple topology and, in order to reduce the structure cost, it is non-isolated from the utility grid.

CML converters have the advantage of reducing the current rating needs for the semiconductor devices, since the main current is shared by a number of paralleled cells. This benefit is worthier for high power applications, although low power CML systems could be employed using small rated (and often cheaper, as well as easily available) devices.

II. A PHOTOVOLTAIC SYSTEM BASED ON THE CURRENT MULTILEVEL BOOST CONVERTER

Fig. 2 shows a single-phase, five-level, current-source CML inverter. This structure employs 8 unidirectional switching devices in such a way the input current is shared by its two-cell arrangement [10]. This system is able to provide a high power factor current injected into the grid and could be used in a photovoltaic approach. However, the need a great number of controllable switches and an input current harmonic spectrum, which includes low frequency components, restricts its practical use.

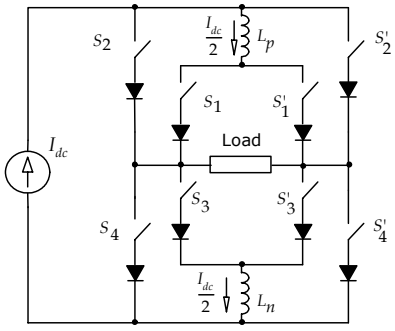

Fig. 2 – Five-level CML current-source inverter.

The CML technique can also be applied to high power factor rectifiers. A high power factor, single-phase rectifier, based on the CML Buck converter [11], has been developed, and is shown in Fig. 3 [12], [13], [16].

The rectifier is able to provide up to five levels for the input current, with low harmonic distortion and unity displacement factor, yielding a high power factor operation. Due to the presence of the CML buck converter, connected in cascade with a conventional diode bridge, this topology is referenced as "Five-Level CML Buck Rectifier". The related rectifier has lead to a new inverter topology, based on the CML Boost Converter, which is proposed in this work. This structure, named "Five-Level CML Boost Inverter", is built with a two-cell CML boost converter (switched with 120 Hz) cascaded by a line-commutated CSI. This arrangement is able to synthesize a five-level current waveform, with low harmonic distortion, as depicted by the idealized waveforms in Fig. 4. The application of this inverter on a PV energy processing system is shown in Fig. 5. Comparing to the CSI shown in Fig. 2, the inverter system of Fig. 5 has the advantage of employing only two self-commutated switches and four thyristors (spontaneous blocking). Since this topology provides an equalized current distribution between the boost converter components, the two-cell CSI structure can also allow the use of lower-rated switches to process a higher current.

A. Mathematical Analysis

Deriving theoretical relationships can be made simpler by assuming some idealized conditions. Thus, it will be assumed a system steady state operation, ideal voltage across the PV panel output, ideal components and negligible ripple on inductor currents. Finally, it is also assumed that the currents that flow through the input inductor L_i and the balance inductor L_b are equal to I and I/2, respectively. The boost CML converter operation is divided in five stages, according to switches S_1 and S_2 conduction states. Table I brings a summary of these operation stages, whose equivalent circuits are shown in the Fig. 6.

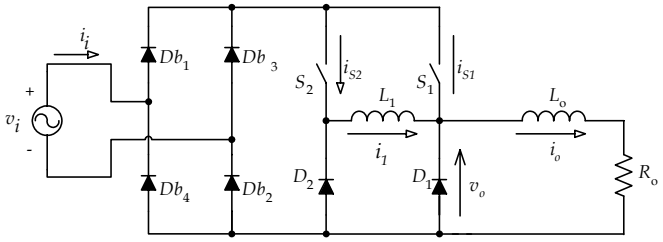

Fig. 3 – Five-level CML Buck rectifier.

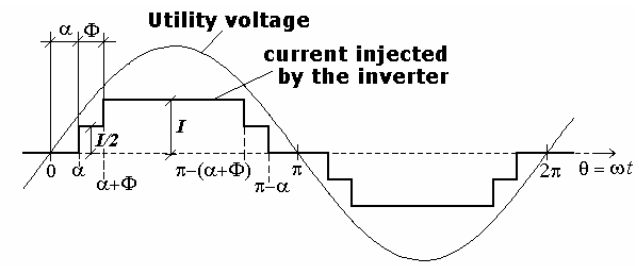

Fig. 4 – Idealized five-level waveform.

Table I – Boost CML operation stages summary.

Stage	S_1	S_2	Interval*
I	ON	ON	$0 \le \theta < \alpha$
II	OFF	ON	$\alpha \le \theta < \alpha+\Phi$
III	OFF	OFF	$\alpha+\Phi \le \theta < \pi-(\alpha+\Phi)$
IV	ON	OFF	$\pi-(\alpha+\Phi) \le \theta < \pi-\alpha$
V	ON	ON	$\pi-\alpha \le \theta < 2\pi$

*see Fig. 4.

Some important relationships can be obtained from these operation stages of the converter. The average and rms values of the current into switch S_1 are given, respectively, by equations (1) and (2).

$$I_{S1} = \frac{(2\alpha+\Phi)}{2\pi} I \tag{1}$$

$$I_{S1}^{rms} = \frac{I}{2}\sqrt{\frac{(2\alpha+\Phi)}{\pi}} \tag{2}$$

The peak voltage across S_1 is equal to the peak of the line voltage. Assuming the line voltage as $v_S = \sqrt{2}V\sin(2\pi f t)$, the average value of the voltage across S_1 is given by:

$$V_{S1} = \frac{\sqrt{2}V}{\pi}\left[\cos(\alpha)+\cos(\alpha+\Phi)\right] \tag{3}$$

where V is the line voltage rms value.

Due to the symmetric operation of the two switches, these equations also applies to switch S_2.

The maximum reverse voltage across the diodes D_1 and D_2 is $\sqrt{2}V\sin(\alpha+\Phi)$ and their average current can be calculated by:

$$I_{D1} = I_{D2} = \frac{(\pi-\Phi)I}{2\pi}. \tag{4}$$

Regarding thyristors, the maximum reverse voltage is equal to the peak of the line voltage. Their average current can be expressed as:

$$I_T = \frac{3I}{4\pi}(\pi-2\alpha-2\Phi). \tag{5}$$

I

Inductor design can be accomplished by linearizing the inductance classical expression:

$$v = L\frac{di}{dt} \approx L\frac{\Delta i}{\Delta t}. \tag{6}$$

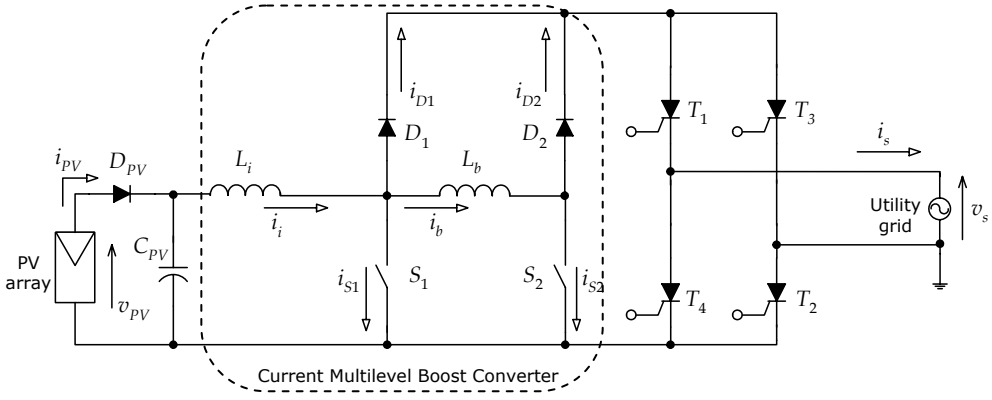

Fig. 5 – Five-level CML Boost Inverter.

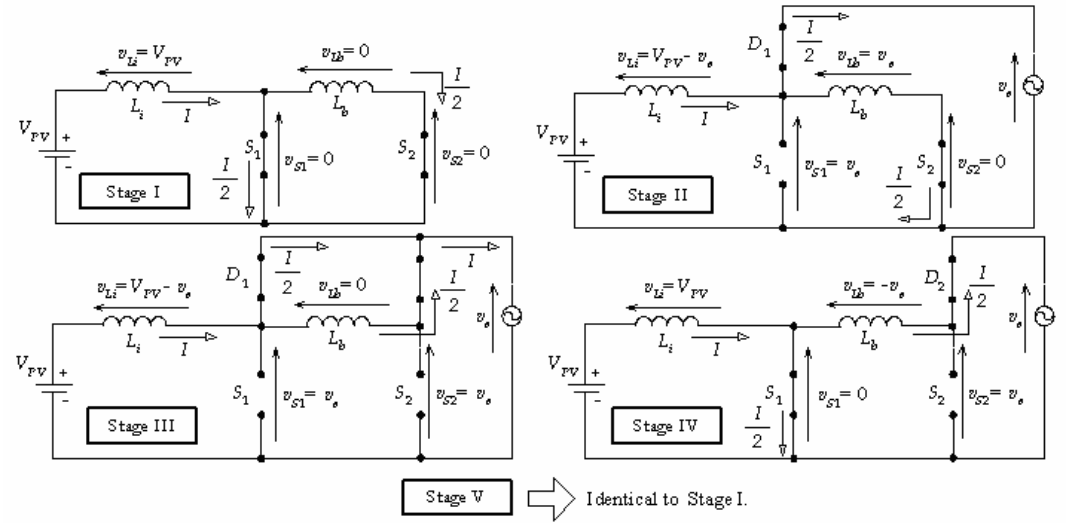

Fig. 6 – Equivalent circuits for each Boost CML operation stage.

Assuming Δi_i is the total ripple on the current trough L_i and Δt, that is a function of α and Φ, is the time interval associated to this current ripple, inductor L_i value can be calculated by:

$$L_i = \frac{V_{PV}(2\alpha + \Phi)}{2\pi f \Delta i_i} \quad (7)$$

where f is the frequency of the line voltage and V_{PV} is the ideal output voltage of the PV panel (see Fig. 6).

Similarly, for the balance inductor L_b,

$$L_b = \frac{\sqrt{2}V[\cos(\alpha) - \cos(\alpha + \Phi)]}{2\pi f \Delta i_b} \quad (8)$$

where Δi_b is the total ripple on the current trough L_b.

The h-th harmonic of the current shown in Fig. 4 is given by equation (9) [12], [16], which is only valid for an odd h. The minimum THD of this current is about 16 %, associated to the angles α = 12.9 ° and Φ = 29.4 ° [16].

$$I_h = \frac{2I}{h\pi}\{\cos(h\alpha) + \cos[h(\alpha + \Phi)]\} \quad (9)$$

B. Photovoltaic Panel Model

In order to obtain more accurate simulation results of the power conditioning setup, a circuit-oriented model [15] of the PV panel BP SX-120 [14] has been developed in Pspice®, as shown in Fig. 7(a). The simulated current-voltage output characteristic is presented in Fig. 7(b).

C. Simulation Results

The photovoltaic system of Fig. 5 has been simulated in Pspice®, employing six PV panels (two groups of three series-connected panels, associated in parallel), providing 720 peak-Watts (Wp) to the system [14]. The system simulation parameters have been set as follows: L_i = 300 mH, L_b = 250 mH, V_s = 127 $V_{(rms)}$, f = 60 Hz. In order to minimize the panel voltage ripple, thereby making easier the implementation of a maximum power point tracking system, a filter capacitor C_{PV} = 1000 µF has been added to the converter input. It is important to consider that the proposed topology can also work without this capacitor. However, its utilization provides an optimization of the PV energy conversion system. Its value can be lower on the expense of a higher voltage ripple. The angles α = 12.6° and Φ = 29.2° (see Fig. 4) have been used to gate switches S_1 and S_2. It is interesting to note that the energy is injected into the grid when at least one of switches S_1 and S_2 is blocked, and an equalized current distribution between them has been achieved. The simulation results are shown in Fig. 8. The obtained total harmonic distortion of the current injected into the grid was 16.4 %, resulting in a power factor closer than 0.99 (zero displacement power factor). The harmonic spectrum of this current is plotted in Fig. 9.

III. HARMONIC OPTIMIZATION SWITCHING STRATEGY

According to IEEE Std. 929-2000 [9], a grid-connected PV system should present low current-distortion levels to ensure that no adverse effects are caused to other equipment connected to the utility system. The harmonic characteristics of the inverter must comply with Clause 10 of IEEE Std. 519-1992 [17], which depends on the short-circuit level at the point of common coupling. For a general case, the IEEE Std. 929-2000 recommends that the total harmonic current distortion shall be less than 5 % at rated inverter output.

In order to improve the harmonic content of the output current in the Five-level CML Boost Inverter, a sinusoidal pulse-width modulation (PWM) can be applied to the system. The only changes required to implement a PWM technique in the system are the gate pulses of switches S_1 and S_2 and the addition of a small low-pass second-order LC filter in the inverter output.

Switch pulse generation has been achieved by comparing a rectified sinusoidal waveform with two 180° out of phase high frequency triangular carriers, performing the pulse-width modulation [18]. To aid visualization, Fig. 10 shows these waveforms for a switching frequency of 600 Hz and amplitude modulation ratio equals to 0.9. The current waveform synthesized in the inverter output has five levels and a carrier frequency of twice the switching frequency (of S_1 or S_2). The inverter only responds for the polarity inversion of the dc waveform generated by the Boost CML converter. Thus it can continue to be a line-commutated inverter. The most important waveforms of the circuit, in the same PV panel configuration of the previous simulation, are presented in Fig. 11. The harmonic spectrum of the current injected into the grid is shown in Fig. 12 (for the 30 first harmonics). High order harmonics are considerably minimized due to the use of the low-pass filter.

(a)

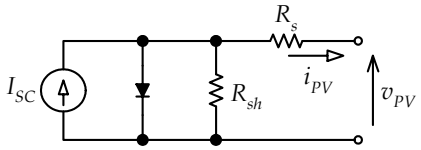

(b)

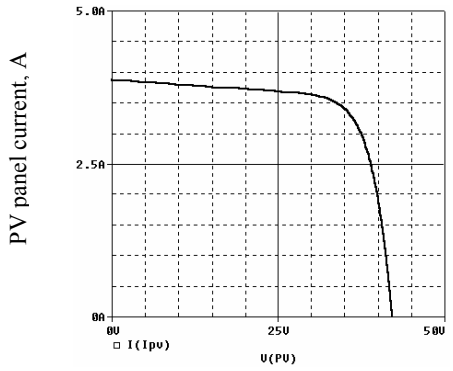

Fig. 7 – Photovoltaic panel model
(a) Equivalent circuit; (b) Output *i-v* characteristic.

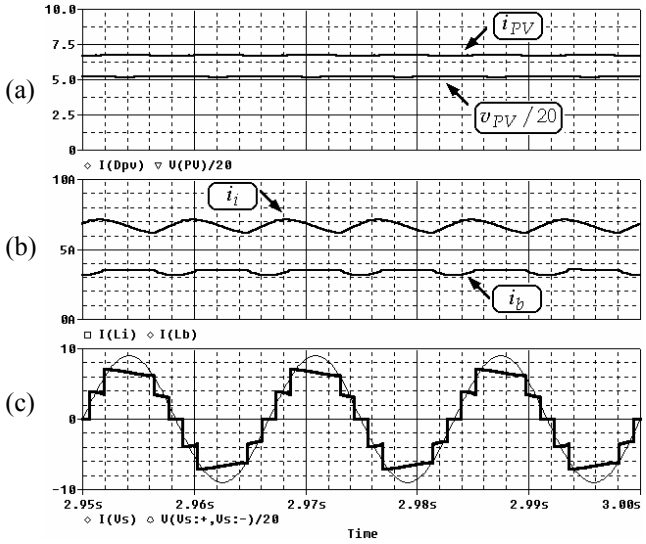

Fig. 8 – Five-Level Boost CML Inverter simulated waveforms. (a) PV panel output current and voltage (voltage scale reduced in 20 times); (b) Current flowing through L_i and L_b; (c) Current injected into the grid (thick trace) and line voltage (thinner trace with scale reduced in 20 times).

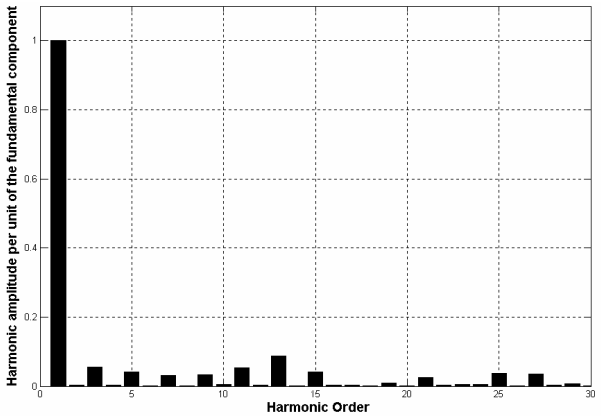

Fig. 9 – Harmonic spectrum of the current inject into the grid.

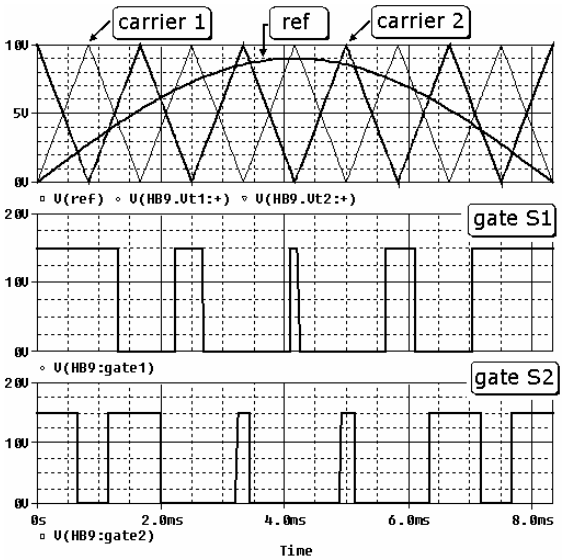

Fig. 10 – PWM switching strategy (just for visualization purposes).

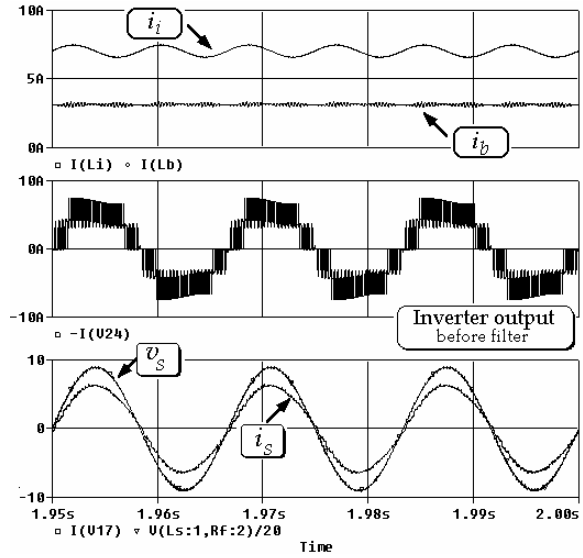

Fig. 11 – Simulated waveforms for PWM operation of the Five-Level Boost CML Inverter.

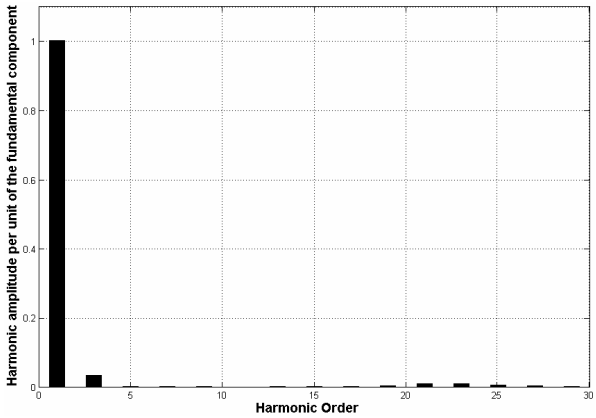

Fig. 12 – Harmonic spectrum of the current inject into the grid.

In order to compensate the lack of experimental results, it has been included in the simulated system a number of practical parasitic elements, such as inductor series resistances and utility stray inductance. Series resistance of input inductor was of 1 Ω, while the balance inductor counterpart was of 0.5 Ω. On the other hand, the stray inductance employed was of 0.5 mH.

It has been achieved for this simulation a THD lower than 4.69 % with a lagging angle of 1.41° between current and line voltage. The system simulation parameters have been set as follows: $L_i = 250$ mH, $L_b = 50$ mH, $V_s = 127\ V_{(rms)}$, $f = 60$ Hz and $f_{SW} = 3$ kHz (carrier frequency). A high frequency second-order filter has been employed, using L = 2.5 mH, C = 4.7 µF and R = 3.3 Ω (line inductor associated with a C-R branch in parallel with the utility voltage).

Note that the input inductance has a value near the one used in the previous situation (Section II.C and Fig. 8). On the other hand, the balance inductance value can be considerably reduced due to the higher frequency adopted. A value below 20 mH has been tested with no significant loss of quality, neither in the multilevel current nor in the filtered one.

III. CONCLUSION

This paper introduced a new current multilevel inverter topology that can be applied to photovoltaic systems. The topology is still unpublished and merges the main advantages of the line-commutated approaches (including high efficiency) and the high-frequency alternatives (low harmonic distortion and high power factor). The low-frequency characteristic of the system makes its implementation easier than most of high-frequency energy processing setups. Another interesting characteristic of the proposed system is its natural ability of short-circuit protection.

The proposed system could be used in residential applications as well as in higher power applications. The multilevel operation becomes more attractive in the latter case, due to the balanced distribution of the total system current among the boost semiconductor devices, allowing the use of small-rated elements. Moreover, the employing of low-frequency switching would allow the use of slower components, e.g. first generation IGBT's for the boost converter, and conventional thyristors for the current source inverter.

The PWM switching strategy makes possible the improvement of the current harmonic content, employing a relatively low switching frequency. It allows a high efficiency operation of the system.

Authors are working now on the experimental validation of the concepts described in this paper. Results will be available in future articles.

IV. REFERENCES

[1] M. Calais, J. Myrzik, T. Spooner, V. G. Agelidis, "Inverters for Single-Phase Grid Connected Photovoltaic Systems - An Overview", in *Proceedings of the 33rd Power Electronics Specialists Conference (PESC'2002)*, Vol. 4, pp 1995-2000, 2002.

[2] Y. B. Blauth, J. O. Wisbeck, A. Krenzinger, "Condicionador de Energia para Painéis Solares com Melhoria do Conteúdo Harmônico e do Fator de Potência da Instalação", in *Anais do XIV Congresso Brasileiro de Automática (CBA 2002)*, pp. 251-256, Natal, September, 2002 (in Portuguese).

[3] J. A. Gow, C. D. Manning, "Photovoltaic Converter System Suitable for Use in Small Scale Stand-Alone or Grid Connected Applications", in *IEE Proc. on Electr. Power Appl.*, vol. 147, no. 6, pp. 535-543, November, 2000.

[4] D. C. Martins, R. Demonti, I. Barbi, "Static Conversion System for Treatment of the Solar Energy and Interconnection with the Mains Power Supply", in *CD-ROM of the V Brazilian Power Electronics Conference (COBEP 99)*, Foz do Iguaçu, 1999.

[5] D. C. Martins, R. Demonti, "Photovoltaic Energy Processing for Utility Connected System", in *Proceeding of the VI Brazilian Power Electronics Conference (COBEP 2001)*, pp. 735-739, Florianópolis, November, 2001.

[6] M. Andersen, B. Alvsten, "200 W Low Cost Module Integrated Utility Interface for Modular Photovoltaic Energy Systems", *Proceedings of the 21st IEEE IECON (IECON 1995)*, pp. 572-577, 1995.

[7] Y. C. Kuo, T. J. Liang, J. F. Chen, "Novel Maximum Power-Point-Tracking Controller for Photovoltaic energy Conversion System", *IEEE Transactions on Industrial Electronics*, Vol. 48, No. 3, pp. 594-601, June, 2001.

[8] K. Souza, S. Daher, F. M. Antunes, "A Single-Phase Inverter for PV Systems", in *Proceedings of the VI Brazilian Power Electronics Conference (COBEP 2001)*, pp. 215-219, Florianópolis, November, 2001.

[9] IEEE Std 929-2000, "IEEE Recommended Practice for Utility Interface of Photovoltaic (PV) Systems", 2000.

[10] F. M. Antunes, H. A. C. Braga, I. Barbi, "Application of a Generalized Current Multilevel Cell to Current-Source Inverters", *IEEE Transactions on Industrial Electronics*, vol. 46, no.1, pp. 31-38, February, 1999.

[11] H. A. C. Braga, I. Barbi, "Current Multilevel DC-DC Converters", in *Procedings of the III Brazilian Power Electronics Conference (COBEP'95)*, pp. 417-422, São Paulo, December, 1995..

[12] E. C. Teixeira, H. A. C. Braga, "A High Power Factor Single-Phase Rectifier Based on a Current Multilevel Buck Converter", in *Proceedings of the VI Brazilian Power Electronics Conference (COBEP 2001)*, pp. 180-185, Florianópolis, November, 2001.

[13] E. C. Teixeira, H. A. C. Braga, "Um Retificador Monofásico com Elevado Fator de Potência Baseado no Conversor Buck Multinível em Corrente", *Revista Eletrônica de Potência*, Sociedade Brasileira de Eletrônica de Potência (SOBRAEP), Vol. 7, No. 1, pp. 62-70. Novembro, 2002 (in Portuguese).

[14] BP SX 120 datasheet, available at http://www.bpsolar.com/ContentDocuments/123/BP_SX_120_Data_Sheet.pdf, 2003.

[15] E. Koutroulis, K. Kalaitzakis, N. C. Voulgaris, "Development of a Microcontroller-Based, Photovoltaic Maximum Power Point Tracking Control System", *IEEE Transactions on Power Electronics*, vol. 15, no.1, pp. 46-54, January, 2001.

[16] E. C. Teixeira, "Retificador Monofásico de Elevado Fator de Potência Baseado no Conversor Buck Multinível em Corrente", Master Thesis, Faculdade de Engenharia - UFJF, *Universidade Federal de Juiz de Fora*, 2002 (in Portuguese).

[17] IEEE Std 519-1992, "IEEE Guide for Harmonic Control and Reactive Compensation of Static Power Converters", 1992.

[18] P. G. Barbosa, "Compensador Série Síncrono Estático Baseado em Conversores VSI Mutipulso", Doctoral Dissertation, COPPE – UFRJ, *Universidade Federal do Rio de Janeiro*, 2000 (in Portuguese).